BELLE-CONF-0566
LP2005-201
EPS05-541

Search for $B \to \tau\nu$ and $B \to K\nu\bar{\nu}$ Decays with a Fully Reconstructed B at Belle

K. Abe,[9] K. Abe,[47] I. Adachi,[9] H. Aihara,[49] K. Aoki,[23] K. Arinstein,[2] Y. Asano,[54] T. Aso,[53] V. Aulchenko,[2] T. Aushev,[13] T. Aziz,[45] S. Bahinipati,[5] A. M. Bakich,[44] V. Balagura,[13] Y. Ban,[36] S. Banerjee,[45] E. Barberio,[22] M. Barbero,[8] A. Bay,[19] I. Bedny,[2] U. Bitenc,[14] I. Bizjak,[14] S. Blyth,[25] A. Bondar,[2] A. Bozek,[29] M. Bračko,[9,21,14] J. Brodzicka,[29] T. E. Browder,[8] M.-C. Chang,[48] P. Chang,[28] Y. Chao,[28] A. Chen,[25] K.-F. Chen,[28] W. T. Chen,[25] B. G. Cheon,[4] C.-C. Chiang,[28] R. Chistov,[13] S.-K. Choi,[7] Y. Choi,[43] Y. K. Choi,[43] A. Chuvikov,[37] S. Cole,[44] J. Dalseno,[22] M. Danilov,[13] M. Dash,[56] L. Y. Dong,[11] R. Dowd,[22] J. Dragic,[9] A. Drutskoy,[5] S. Eidelman,[2] Y. Enari,[23] D. Epifanov,[2] F. Fang,[8] S. Fratina,[14] H. Fujii,[9] N. Gabyshev,[2] A. Garmash,[37] T. Gershon,[9] A. Go,[25] G. Gokhroo,[45] P. Goldenzweig,[5] B. Golob,[20,14] A. Gorišek,[14] M. Grosse Perdekamp,[38] H. Guler,[8] R. Guo,[26] J. Haba,[9] K. Hara,[9] T. Hara,[34] Y. Hasegawa,[42] N. C. Hastings,[49] K. Hasuko,[38] K. Hayasaka,[23] H. Hayashii,[24] M. Hazumi,[9] T. Higuchi,[9] L. Hinz,[19] T. Hojo,[34] T. Hokuue,[23] Y. Hoshi,[47] K. Hoshina,[52] S. Hou,[25] W.-S. Hou,[28] Y. B. Hsiung,[28] Y. Igarashi,[9] T. Iijima,[23] K. Ikado,[23] A. Imoto,[24] K. Inami,[23] A. Ishikawa,[9] H. Ishino,[50] K. Itoh,[49] R. Itoh,[9] M. Iwasaki,[49] Y. Iwasaki,[9] C. Jacoby,[19] C.-M. Jen,[28] R. Kagan,[13] H. Kakuno,[49] J. H. Kang,[57] J. S. Kang,[16] P. Kapusta,[29] S. U. Kataoka,[24] N. Katayama,[9] H. Kawai,[3] N. Kawamura,[1] T. Kawasaki,[31] S. Kazi,[5] N. Kent,[8] H. R. Khan,[50] A. Kibayashi,[50] H. Kichimi,[9] H. J. Kim,[18] H. O. Kim,[43] J. H. Kim,[43] S. K. Kim,[41] S. M. Kim,[43] T. H. Kim,[57] K. Kinoshita,[5] N. Kishimoto,[23] S. Korpar,[21,14] Y. Kozakai,[23] P. Križan,[20,14] P. Krokovny,[9] T. Kubota,[23] R. Kulasiri,[5] C. C. Kuo,[25] H. Kurashiro,[50] E. Kurihara,[3] A. Kusaka,[49] A. Kuzmin,[2] Y.-J. Kwon,[57] J. S. Lange,[6] G. Leder,[12] S. E. Lee,[41] Y.-J. Lee,[28] T. Lesiak,[29] J. Li,[40] A. Limosani,[9] S.-W. Lin,[28] D. Liventsev,[13] J. MacNaughton,[12] G. Majumder,[45] F. Mandl,[12] D. Marlow,[37] H. Matsumoto,[31] T. Matsumoto,[51] A. Matyja,[29] Y. Mikami,[48] W. Mitaroff,[12] K. Miyabayashi,[24] H. Miyake,[34] H. Miyata,[31] Y. Miyazaki,[23] R. Mizuk,[13] D. Mohapatra,[56] G. R. Moloney,[22] T. Mori,[50] A. Murakami,[39] T. Nagamine,[48] Y. Nagasaka,[10] T. Nakagawa,[51] I. Nakamura,[9] E. Nakano,[33] M. Nakao,[9] H. Nakazawa,[9] Z. Natkaniec,[29] K. Neichi,[47] S. Nishida,[9] O. Nitoh,[52] S. Noguchi,[24] T. Nozaki,[9] A. Ogawa,[38] S. Ogawa,[46] T. Ohshima,[23] T. Okabe,[23] S. Okuno,[15] S. L. Olsen,[8] Y. Onuki,[31] W. Ostrowicz,[29] H. Ozaki,[9] P. Pakhlov,[13] H. Palka,[29] C. W. Park,[43] H. Park,[18] K. S. Park,[43] N. Parslow,[44] L. S. Peak,[44] M. Pernicka,[12] R. Pestotnik,[14] M. Peters,[8] L. E. Piilonen,[56] A. Poluektov,[2] F. J. Ronga,[9] N. Root,[2] M. Rozanska,[29] H. Sahoo,[8] M. Saigo,[48] S. Saitoh,[9] Y. Sakai,[9] H. Sakamoto,[17] H. Sakaue,[33] T. R. Sarangi,[9] M. Satapathy,[55] N. Sato,[23] N. Satoyama,[42] T. Schietinger,[19] O. Schneider,[19] P. Schönmeier,[48] J. Schümann,[28] C. Schwanda,[12] A. J. Schwartz,[5] T. Seki,[51] K. Senyo,[23] R. Seuster,[8] M. E. Sevior,[22] T. Shibata,[31] H. Shibuya,[46] J.-G. Shiu,[28] B. Shwartz,[2] V. Sidorov,[2] J. B. Singh,[35] A. Somov,[5] N. Soni,[35] R. Stamen,[9] S. Stanič,[32] M. Starič,[14] A. Sugiyama,[39] K. Sumisawa,[9] T. Sumiyoshi,[51] S. Suzuki,[39] S. Y. Suzuki,[9] O. Tajima,[9] N. Takada,[42] F. Takasaki,[9] K. Tamai,[9] N. Tamura,[31] K. Tanabe,[49] M. Tanaka,[9] G. N. Taylor,[22] Y. Teramoto,[33] X. C. Tian,[36] K. Trabelsi,[8]

Y. F. Tse,[22] T. Tsuboyama,[9] T. Tsukamoto,[9] K. Uchida,[8] Y. Uchida,[9] S. Uehara,[9] T. Uglov,[13] K. Ueno,[28] Y. Unno,[9] S. Uno,[9] P. Urquijo,[22] Y. Ushiroda,[9] G. Varner,[8] K. E. Varvell,[44] S. Villa,[19] C. C. Wang,[28] C. H. Wang,[27] M.-Z. Wang,[28] M. Watanabe,[31] Y. Watanabe,[50] L. Widhalm,[12] C.-H. Wu,[28] Q. L. Xie,[11] B. D. Yabsley,[56] A. Yamaguchi,[48] H. Yamamoto,[48] S. Yamamoto,[51] Y. Yamashita,[30] M. Yamauchi,[9] Heyoung Yang,[41] J. Ying,[36] S. Yoshino,[23] Y. Yuan,[11] Y. Yusa,[48] H. Yuta,[1] S. L. Zang,[11] C. C. Zhang,[11] J. Zhang,[9] L. M. Zhang,[40] Z. P. Zhang,[40] V. Zhilich,[2] T. Ziegler,[37] and D. Zürcher[19]

(The Belle Collaboration)

[1]*Aomori University, Aomori*
[2]*Budker Institute of Nuclear Physics, Novosibirsk*
[3]*Chiba University, Chiba*
[4]*Chonnam National University, Kwangju*
[5]*University of Cincinnati, Cincinnati, Ohio 45221*
[6]*University of Frankfurt, Frankfurt*
[7]*Gyeongsang National University, Chinju*
[8]*University of Hawaii, Honolulu, Hawaii 96822*
[9]*High Energy Accelerator Research Organization (KEK), Tsukuba*
[10]*Hiroshima Institute of Technology, Hiroshima*
[11]*Institute of High Energy Physics, Chinese Academy of Sciences, Beijing*
[12]*Institute of High Energy Physics, Vienna*
[13]*Institute for Theoretical and Experimental Physics, Moscow*
[14]*J. Stefan Institute, Ljubljana*
[15]*Kanagawa University, Yokohama*
[16]*Korea University, Seoul*
[17]*Kyoto University, Kyoto*
[18]*Kyungpook National University, Taegu*
[19]*Swiss Federal Institute of Technology of Lausanne, EPFL, Lausanne*
[20]*University of Ljubljana, Ljubljana*
[21]*University of Maribor, Maribor*
[22]*University of Melbourne, Victoria*
[23]*Nagoya University, Nagoya*
[24]*Nara Women's University, Nara*
[25]*National Central University, Chung-li*
[26]*National Kaohsiung Normal University, Kaohsiung*
[27]*National United University, Miao Li*
[28]*Department of Physics, National Taiwan University, Taipei*
[29]*H. Niewodniczanski Institute of Nuclear Physics, Krakow*
[30]*Nippon Dental University, Niigata*
[31]*Niigata University, Niigata*
[32]*Nova Gorica Polytechnic, Nova Gorica*
[33]*Osaka City University, Osaka*
[34]*Osaka University, Osaka*
[35]*Panjab University, Chandigarh*
[36]*Peking University, Beijing*
[37]*Princeton University, Princeton, New Jersey 08544*

[38]RIKEN BNL Research Center, Upton, New York 11973
[39]Saga University, Saga
[40]University of Science and Technology of China, Hefei
[41]Seoul National University, Seoul
[42]Shinshu University, Nagano
[43]Sungkyunkwan University, Suwon
[44]University of Sydney, Sydney NSW
[45]Tata Institute of Fundamental Research, Bombay
[46]Toho University, Funabashi
[47]Tohoku Gakuin University, Tagajo
[48]Tohoku University, Sendai
[49]Department of Physics, University of Tokyo, Tokyo
[50]Tokyo Institute of Technology, Tokyo
[51]Tokyo Metropolitan University, Tokyo
[52]Tokyo University of Agriculture and Technology, Tokyo
[53]Toyama National College of Maritime Technology, Toyama
[54]University of Tsukuba, Tsukuba
[55]Utkal University, Bhubaneswer
[56]Virginia Polytechnic Institute and State University, Blacksburg, Virginia 24061
[57]Yonsei University, Seoul

Abstract

We present a search for the decays $B^- \to \tau^- \overline{\nu}$ and $B^- \to K^- \nu \overline{\nu}$ in a 253 fb^{-1} data sample collected at the $\Upsilon(4S)$ resonance with the Belle detector at the KEKB asymmetric energy B factory. Combinatorial and continuum backgrounds are suppressed by selecting a sample of events with one fully reconstructed B. The decay products of the B on the other side of the event are analyzed to search for $B^- \to \tau^- \overline{\nu}$ and $B^- \to K^- \nu \overline{\nu}$ decays. We find no significant evidence for a signal and set 90% confidence level upper limits of $\mathcal{B}(B^- \to \tau^- \overline{\nu}) < 1.8 \times 10^{-4}$ and $\mathcal{B}(B^- \to K^- \nu \overline{\nu}) < 3.6 \times 10^{-5}$. All results are preliminary.

PACS numbers:

The purely leptonic decay $B^- \to \ell^- \overline{\nu}$ (charge conjugate states are implied throughout the paper) is of particular interest since it provides direct measurement of the product of the Cabibbo-Kobayashi-Maskawa(CKM) matrix element V_{ub} and the B meson decay constant f_B. In the Standard Model(SM), the branching fraction of the decay $B^- \to \ell^- \overline{\nu}$ is given as

$$\mathcal{B}(B^- \to \ell^- \overline{\nu}) = \frac{G_F^2 m_B m_\ell^2}{8\pi} \left(1 - \frac{m_\ell^2}{m_B^2}\right)^2 f_B^2 |V_{ub}|^2 \tau_B \quad (1)$$

where G_F is the Fermi coupling constant, m_ℓ and m_B are the charged lepton and B meson masses, τ_B is the B^- lifetime. The dependence on the lepton mass arises from helicity conservation, which suppresses the muon and electron channels. The CKMfitter predicts the $B^- \to \tau^- \bar{\nu}$ branching fraction to be $(9.3^{+3.4}_{-2.3}) \times 10^{-5}$[1]. No evidence for an enhancement relative to the SM prediction was observed in previous experimental studies. The most stringent upper limit has been achieved by the BABAR Collaboration : $\mathcal{B}(B^- \to \tau^- \overline{\nu}) < 4.2 \times 10^{-4}$ at 90% confidence level (C.L.) [2].

Flavor-changing neutral-current transition such as $b \to s\nu\bar{\nu}$ occurs in the SM via one-loop box or electroweak penguin diagrams with heavy particles in the loops. Because heavy non-SM particles could contribute additional loop diagrams, various new physics scenarios can lead to significant enhancements in the observed rates [3, 4]. The SM $B^- \to K^- \nu\bar{\nu}$ branching fraction has been estimated to be $(3.8^{+1.2}_{-0.6}) \times 10^{-6}$[5, 6], while the most stringent published experimental limit is $\mathcal{B}(B^- \to K^- \nu\overline{\nu}) < 5.2 \times 10^{-5}$ at 90% C.L. [7]

We use a 253 fb^{-1} data sample containing 275×10^6 B meson pairs collected with the Belle detector at the KEKB asymmetric energy e^+e^- (3.5 on 8 GeV) collider [8] operating at the $\Upsilon(4S)$ resonance ($\sqrt{s} = 10.58$ GeV). The Belle detector is a large-solid-angle magnetic spectrometer consisting of a three-layer silicon vertex detector, a 50-layer central drift chamber (CDC), a system of aerogel threshold Čerenkov counters (ACC), time-of-flight scintillation counters (TOF), and an electromagnetic calorimeter comprised of CsI(Tl) crystals (ECL) located inside a superconducting solenoid coil that provides a 1.5 T magnetic field. An iron flux-return located outside of the coil is instrumented to identify K_L^0 and muons. The detector is described in detail elsewhere [9].

The strategy adopted for this analysis is to reconstruct exclusively the decay of one of the B mesons in the event and compare properties of the remaining particle(s) in the event (referred to as the signal side) to those expected for signal and background. All the tracks and photon candidates in the event not used to reconstruct the B are studied to search for $B^- \to \tau^- \overline{\nu}$ and $B^- \to K^- \nu\overline{\nu}$. The advantage of having a sample of fully reconstructed B meson is to provide a strong suppression of the combinatorial and continuum background events. The disadvantage is the low efficiency of full B meson reconstruction (approximately 0.3%).

Fully reconstructed B mesons, $B_{\rm rec}$, are observed in the following decay modes: $B^+ \to \overline{D}^{(*)0}\pi^+$, $\overline{D}^{(*)0}\rho^+$, $\overline{D}^{(*)0}a_1^+$ and $\overline{D}^{(*)0}D_s^{(*)+}$ where ρ^+ is reconstructed in $\pi^+\pi^0$ mode ($|M_{\pi^+\pi^0} - M_{\rho^+}| < 0.3$ GeV/c^2) and a_1^+ is reconstructed as $a_1^+ \to \rho^0\pi^+$ ($|M_{\rho^0\pi^+} - M_{a_1^+}| < 0.25$ GeV/c^2). $\overline{D}^0$ candidates are reconstructed as $\overline{D}^0 \to K^+\pi^-$, $K^+\pi^-\pi^0$, $K^+\pi^-\pi^+\pi^-$, $K_S^0\pi^0$, $K_S^0\pi^-\pi^+$, $K_S^0\pi^-\pi^+\pi^0$ and K^-K^+. $\overline{D}^{*0}$ mesons are reconstructed by combining the $\overline{D}^0$ candidates with a pion or a photon. The invariant mass of $\overline{D}^{*0}$ candidates is required to be within a ± 3 MeV/c^2 (for $\overline{D}^{*0}\pi^0$) and ± 10 MeV/c^2 (for $\overline{D}^{*0}\gamma$) intervals around the nominal $\overline{D}^{*0}$ mass. D_s^+ candidates are reconstructed in the decay modes $D_s^+ \to K_S^0K^+$ and $K^+K^-\pi^+$. The invariant mass of the D_s^+ candidates is required to be within ± 15 MeV/c^2 interval

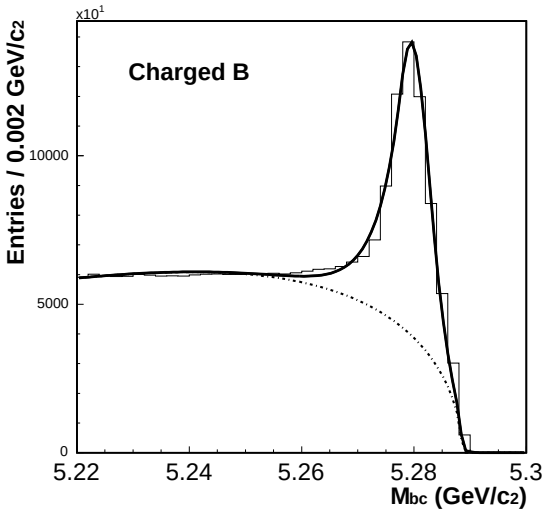

FIG. 1: Distribution of the beam energy constrained mass in data for fully reconstructed B mesons (histogram). The solid curve shows the result of the fit and the dotted one is the background component.

around the nominal D_s^+ mass. D_s^{*+} candidates are defined as $D_s^+\gamma$ combinations where the $D_s^+\gamma$ invariant mass lies in the interval ± 15 MeV/c^2 around the nominal D_s^{*+} mass. Charged B pair events are produced from $\Upsilon(4S)$ resonance ($\sqrt{s} \sim 10.58$ GeV), where the B^+ or B^- is produced with specific momentum and energy. Selection of the fully reconstructed B candidates is made according to the values of two variables : the beam-constrained mass $M_{\rm bc} \equiv \sqrt{E_{\rm beam}^2 - p_B^2}$ and the energy difference $\Delta E \equiv E_B - E_{beam}$. Here, E_B and p_B are the reconstructed energy and momentum of the fully reconstructed B candidate in the center-of-mass (CM) system, and $E_{\rm beam}$ is the beam energy in the CM frame. The signal region for tagging B candidates is defined as $M_{\rm bc} > 5.27$ GeV/c^2 and -80 MeV $< \Delta E < 60$ MeV.

The $M_{\rm bc}$ distribution of reconstructed B candidates is fit with the sum of an Argus function [10] and a Crystal Ball function [11]. The Argus function models the continuum and combinatorial background whereas the Crystal Ball function models the signal component, which peaks at the B mass. The purity is defined as $S/(S+B)$, where S (B) is the number of signal (background) events for $M_{\rm bc} > 5.27$ GeV/c^2, as determined from a fit. Fig. 1 shows the $M_{\rm bc}$ distribution for all $B_{\rm rec}$ candidates in our data set in the signal ΔE region. In this sample, there are cross-feed effects between charged and neutral B. From the Monte Carlo simulation, we estimate the fraction of B^0 (B^+) events in the reconstruction of B^+ (B^0) to be 0.095 (0.090). Then, we obtain $N_{B^+B^-} = (4.00 \pm 0.24) \times 10^5$ and the purity of 0.55, where the uncertainty on $N_{B^+B^-}$ is dominated by systematic errors.

In the events where a $B_{\rm rec}$ is reconstructed, we search for decays into a τ plus a neutrino and a K plus two neutrinos. Candidate events are required to have one or three signal-side charged track(s) with the total charge being opposite to that of the reconstructed B. The τ lepton is identified in the following decay channels: $\tau^- \to \mu^-\nu\bar{\nu}$, $\tau^- \to e^-\nu\bar{\nu}$, $\tau^- \to \pi^-\nu$, $\tau^- \to \pi^-\pi^0\nu$, and $\tau^- \to \pi^-\pi^+\pi^-\nu$.

We require the charged particles to be identified as leptons, pions or kaons. The event is required to have zero net charge and $E_{\rm ECL}$ less than 0.3 GeV where $E_{\rm ECL}$ is the remaining energy calculated by adding the energy of the photons that are not associated with either the $B_{\rm rec}$ or the π^0 candidate from $\tau^- \to \pi^-\pi^0\nu$ decay. For all modes except $\tau^- \to \pi^-\pi^0\nu$

Decay Mode		r_{MC}	Sideband Data	Sideband MC	MC signal region	Expected BG
$B^- \to \tau^- \bar{\nu}$	$\tau^- \to \mu^- \nu \bar{\nu}$	0.17	70	63.9 ± 7.2	10.7 ± 2.8	11.8 ± 3.6
	$\tau^- \to e^- \nu \bar{\nu}$	0.14	67	62.3 ± 8.1	8.9 ± 2.6	9.5 ± 3.2
	$\tau^- \to \pi^- \nu$	0.07	47	48.4 ± 7.7	3.6 ± 1.6	3.5 ± 1.7
	$\tau^- \to \pi^- \pi^0 \nu$	0.23	13	19.2 ± 4.0	4.4 ± 2.1	3.0 ± 1.8
	$\tau^- \to \pi^- \pi^+ \pi^- \nu$	0.23	16	23.0 ± 7.2	5.2 ± 2.5	3.6 ± 2.2
$B^- \to K^- \nu \bar{\nu}$		0.15	17	18.9 ± 4.7	2.9 ± 1.4	2.6 ± 1.6

TABLE I: Expected background in the signal region for the different selection modes.

mode we reject events with π^0 mesons in the recoil against $B_{\rm rec}$.

We place the following requirements on the momentum of the track(s) in the CM, $p_{\pi^-} > 0.8$ GeV/c for $\tau^- \to \pi^- \nu$, $p_{\pi^-\pi^0} > 1.2$ GeV/c for $\tau^- \to \pi^- \pi^0 \nu$, $p_{\pi^-\pi^+\pi^-} > 1.4$ GeV/c for $\tau^- \to \pi^- \pi^+ \pi^- \nu$, and $p_{K^-} > 1.2$ GeV/c for $B^- \to K^- \nu \bar{\nu}$. The event is required to have the total missing momentum of the event to be greater than 0.2 GeV/c for all modes except leptonic decay modes and the direction of missing momentum to be $-0.86 < \cos\theta^*_{\rm miss} < 0.95$ in the CM frame. Further requirements are made on the invariant mass of two or three pions $|M_{\pi\pi} - M_\rho| < 0.15$ GeV/c^2 and $|M_{\pi\pi\pi} - M_{a_1^+}| < 0.2$ GeV/c^2. The selection efficiencies for each decay mode we consider in this analysis are determined from a large sample of GEANT-based Monte Carlo simulations [12] for $B^- \to \tau^- \bar{\nu}$ and $B^- \to K^- \nu \bar{\nu}$ events generated by EvtGen decay package[13]. We compute the efficiency as the ratio of the number of events surviving each of our selections over the number of fully reconstructed $B^\pm$.

The most powerful variable for separating signal and background is the remaining energy $E_{\rm ECL}$. We use different energy cuts for neutral clusters contributing to the $E_{\rm ECL}$ for barrel part and end-cap parts since the effect of beam background is severe in the end-caps. For signal events the neutral clusters contributing to the $E_{\rm ECL}$ can only come from beam background, therefore the signal events peaks at low $E_{\rm ECL}$ and the background events, which contain additional sources of neutral clusters, are distributed toward higher $E_{\rm ECL}$ values.

The $E_{\rm ECL} < 0.3$ GeV region is defined as the signal region and the $0.45 < E_{\rm ECL} < 1.5$ GeV region is defined as the sideband region. The $E_{\rm ECL}$ shape in the MC distribution is used to extrapolate the sideband data to the signal region. The number of MC events in signal region and sideband are counted and their ratio (r_{MC}) is obtained. Using the number of data in the sideband and the ratio r_{MC}, the number of expected background events in the signal region is estimated. The background estimation for the different subdecay modes from the $E_{\rm ECL}$ sideband extrapolation is shown in Table I. The numbers of events in sideband region agrees well between MC and data. To obtain the background expected from the MC simulation, $B\overline{B}$ and $e^+e^- \to u\bar{u},\ d\bar{d},\ s\bar{s},\ c\bar{c}$ events are scaled to equivalent luminosity in data.

The double tag events, for which one of the B mesons is fully reconstructed and the other B meson is reconstructed in the set of decay modes $B^- \to D^0 \ell^- \bar{\nu}$, where ℓ is a muon or an electron and the D^0 is reconstructed in two modes : $D^0 \to K^+\pi^-$ & $K^+\pi^-\pi^+\pi^-$, are used as a control sample to validate the $E_{\rm ECL}$ simulation. The sources affecting the $E_{\rm ECL}$ in double-tagged events are similar to those affecting the $E_{\rm ECL}$ distribution in the signal MC

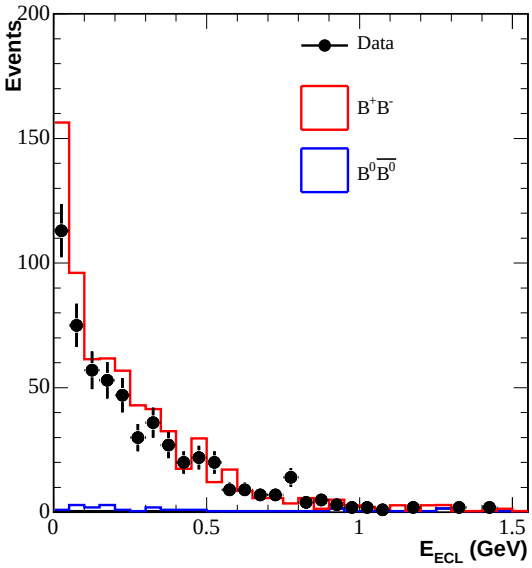

FIG. 2: The $E_{\rm ECL}$ distribution for double-tagged events, plotted for simulation and data. Continuum background is negligible.

simulation. The agreement of the $E_{\rm ECL}$ distribution between data and MC simulation for the double-tagged sample, in Fig. 2, is used as a validation of the $E_{\rm ECL}$ simulation in the signal MC.

The main sources of uncertainty we consider in the determination of the $\mathcal{B}(B^- \to \tau^- \overline{\nu})$ and $\mathcal{B}(B^- \to K^- \nu^- \overline{\nu})$ are the number of B^+B^- events with one reconstructed B, the determination of the signal efficiency and the determination of the number of expected background events. The number of B^+B^- events is determined as the area of the Crystal Ball function fitted to the $M_{\rm bc}$ distribution. Using a Gaussian function as an alternative fitting function, we obtain a relative change in the number of events and this difference is assigned as the systematic uncertainty on the number of B^+B^- events. The main contribution to the systematic uncertainties in the determination of the efficiencies comes from uncertainty on tracking efficiency, Monte Carlo statistics and particle identification. The uncertainty in the expected background comes from Monte Carlo statistics and statistics of sideband data events. Estimates of systematic uncertainties are summarized in Table II.

After finalizing the signal selection criteria, the signal region ($E_{\rm ECL} < 0.3$ GeV) in the on-resonance data is examined. Table III lists the number of observed events in data in the signal region, together with the expected number of signal and background events in the signal region. Fig. 3 shows the $E_{\rm ECL}$ distributions in the data after all selection requirements except the one on $E_{\rm ECL}$ have been applied compared with the expected background. Each distribution refers to a different mode.

Since we do not observe significant excess over the expected background, we set upper limits. To extract the upper limits on the branching fraction for $\mathcal{B}(B^- \to \tau^- \overline{\nu})$ and $\mathcal{B}(B^- \to K^- \nu \overline{\nu})$, we fit the observed $E_{\rm ECL}$ distributions to the expected background and signal, using

Source	Relative uncertainty (%)					
	$\mu^-\nu\bar{\nu}$	$e^-\nu\bar{\nu}$	$\pi^-\nu$	$\pi^-\pi^0\nu$	$\pi^+\pi^-\pi^+\nu$	$K^-\nu\bar{\nu}$
Number of B^+B^-	6.0					
tracking	2.0	2.0	2.0	2.0	6.0	2.0
τ decay BR	0.3	0.3	1.0	0.6	1.1	
MC statistics	0.6	0.6	0.7	1.0	2.0	4.1
Lepton identification	2.2	2.2				
π^0 identification				2.6		
$\pi^\pm$ identification			1.7	1.7	5.1	
Total Efficiency Uncertainty	2.9	2.9	3.0	4.0	8.8	5.0
MC statistics	28.2	31.8	47.5	52.0	57.1	55.8
Data in sideband	12.0	12.2	14.6	27.2	25.0	24.3
Total Background Uncertainty	30.6	34.1	49.7	58.7	62.3	60.9

TABLE II: Systematic uncertainties for the number of B^+B^- events with one reconstructed B, the determination of the efficiency and the determination of the number of expected background events for the different decay channels.

Decay Mode		Signal Efficiency(%)	Signal Expected	Background Expected	Observed Events
$B^- \to \tau^-\bar{\nu}$	$\tau^- \to \mu^-\nu\bar{\nu}$	9.8 ± 0.1	3.9 ± 0.1	11.8 ± 3.6	8
	$\tau^- \to e^-\nu\bar{\nu}$	9.4 ± 0.1	3.8 ± 0.1	9.5 ± 3.2	10
	$\tau^- \to \pi^-\nu$	8.4 ± 0.1	3.4 ± 0.1	3.5 ± 1.7	11
	$\tau^- \to \pi^-\pi^0\nu$	3.5 ± 0.1	1.4 ± 0.1	3.0 ± 1.8	4
	$\tau^- \to \pi^-\pi^+\pi^-\nu$	2.6 ± 0.1	1.0 ± 0.1	3.6 ± 2.2	6
Total		33.7 ± 1.4	13.5 ± 0.2	31.4 ± 5.9	39
$B^- \to K^-\nu\bar{\nu}$		42.8 ± 1.8	0.70 ± 0.03	2.6 ± 1.6	4

TABLE III: Number of observed data events in the signal region, together with number of expected signal and background events. Errors in the background expectation is both statistical and systematic errors. The numbers of expected signal are obtained by assuming that $\mathcal{B}(B^- \to \tau^-\overline{\nu}) = 10^{-4}$ and $\mathcal{B}(B^- \to K^-\nu\overline{\nu}) = 4 \times 10^{-6}$.

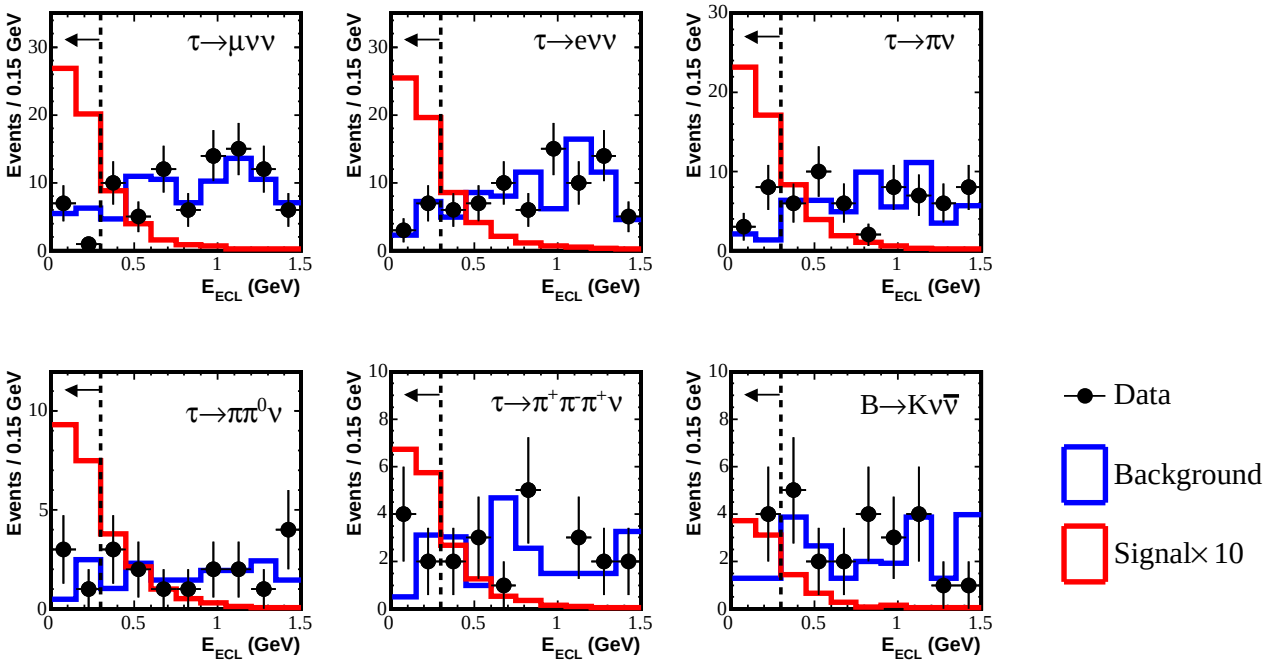

FIG. 3: $E_{\rm ECL}$ distributions in the data after all selection requirements except the one on $E_{\rm ECL}$ have been applied. The red histograms represent the distributions for Monte Carlo simulated signal events scaled to $\mathcal{B}(B^- \to \tau^- \overline{\nu}) = 10^{-4}$ and $\mathcal{B}(B^- \to K^- \nu\overline{\nu}) = 4 \times 10^{-6}$.

maximum likelihood method. The likelihood function $\mathcal{L}$ is defined as

$$\mathcal{L} = \frac{1}{\sqrt{2\pi}\sigma_b} e^{-(n_b - N_b)^2/2\sigma_b} \cdot \frac{e^{-(n_s+n_b)}(n_s+n_b)^N}{N!} \prod_{i=1}^{N} \frac{n_s f_b(i) + n_b f_s(i)}{n_s + n_b}$$

where n_b and n_s represent the number of background and signal events, respectively, N is the number of observed events, N_b is the calculated number of background events, and σ_b is the calculated background uncertainty. The variable f_s is the normalized signal $E_{\rm ECL}$ distribution and f_b is the normalized background $E_{\rm ECL}$ distribution. The negative log likelihood function is minimized using MINUIT [14] with respect to n_b for each n_s $(= \varepsilon_i \cdot N_{B^+B^-} \cdot \mathcal{B})$. The 90% C. L. upper limit on the branching fraction $\mathcal{B}$ is calculated by

$$0.9 = \frac{\int_0^{\mathcal{B}_{90}} \mathcal{L}(\mathcal{B}) d\mathcal{B}}{\int_0^{\infty} \mathcal{L}(\mathcal{B}) d\mathcal{B}} \tag{2}$$

For $B^- \to \tau^- \overline{\nu}$, we calculate the likelihood function for each different decay mode $(\mathcal{L}_i(\mathcal{B}))$. Total likelihood function is defined by

$$\mathcal{L}(\mathcal{B}) = \prod_{i=1}^{n_{ch}} \mathcal{L}_i(\mathcal{B}) \tag{3}$$

where n_{ch} is the number of decay modes for $B^- \to \tau^- \overline{\nu}$. The full systematic uncertainty must be incorporated into the likelihood function. We convolve the systematic uncertainty into the likelihood function, $\mathcal{L}(\mathcal{B})$, by replacing each point of $\mathcal{L}(\mathcal{B})$ by a Gaussian distribution

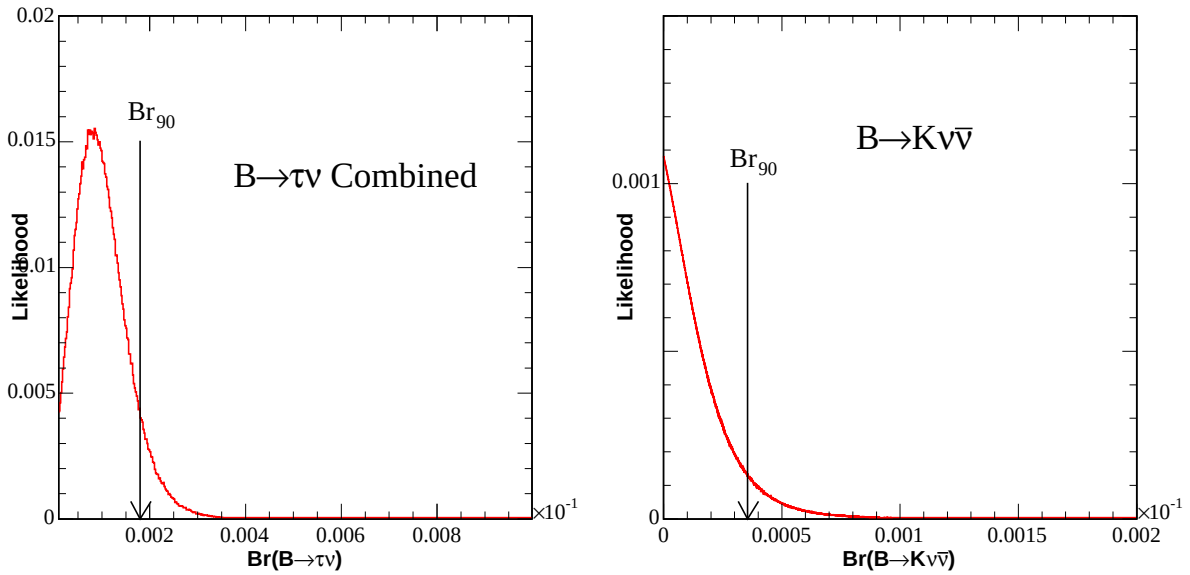

FIG. 4: Likelihood functions for the fit to data after smearing.

centered at that point with width $\Delta\mathcal{B}$ which is determined from systematic uncertainty study. To get the value of a particular point of the smeared likelihood function, we integrate all the contributions from the Gaussian replaced points of the unsmeared likelihood function. To combine likelihood functions of 5 decay modes for $B^- \to \tau^-\overline{\nu}$, we simply multiply the likelihood functions to produce the combined likelihood. The only complication arises in that there are common sources of systematic uncertainty and therefore correlated uncertainties between the samples. We throw different normal Gaussian random number for correlated and uncorrelated systematics for each systematics sources. In this way, we can smear the correlated systematics in the same direction. We obtain the final smeared likelihood function by multiplying smeared likelihood functions for $B^- \to \tau^-\overline{\nu}$. For $B^- \to K^-\nu\overline{\nu}$ decay, we smear the likelihood function by the total systematic uncertainty. Fig. 4 shows the likelihood functions for the fit to data after smearing for $B^- \to \tau^-\overline{\nu}$ (left) and $B^- \to K^-\nu\overline{\nu}$ (right). We obtain upper limits on the branching fraction at the 90% (C.L.) of

$$\mathcal{B}(B^- \to \tau^-\overline{\nu}) < 1.8 \times 10^{-4} \tag{4}$$

$$\mathcal{B}(B^- \to K^-\nu\overline{\nu}) < 3.6 \times 10^{-5}. \tag{5}$$

In the extension of the Standard Model, one expects significant modification to the $B^- \to \tau^-\overline{\nu}$ decay branching fraction. In the two-Higgs doublet model, the decay can occur via a charged Higgs particle. The $B^- \to \tau^-\overline{\nu}$ branching fraction is given as

$$\mathcal{B}(B^- \to \tau^-\overline{\nu}) = \mathcal{B}(B^- \to \tau^-\overline{\nu})_{\rm SM} \times r_H, \tag{6}$$

where r_H is defined as

$$r_H = \left(1 - \frac{\tan^2\beta}{m_H^2} m_B^2\right)^2, \tag{7}$$

m_H is the charged Higgs mass and $\tan\beta$ is the ratio of vacuum expectation values of two Higgs doublets [15]. $\mathcal{B}(B^- \to \tau^-\overline{\nu})_{\rm SM}$ represents SM contribution given by Eq.(1). Once

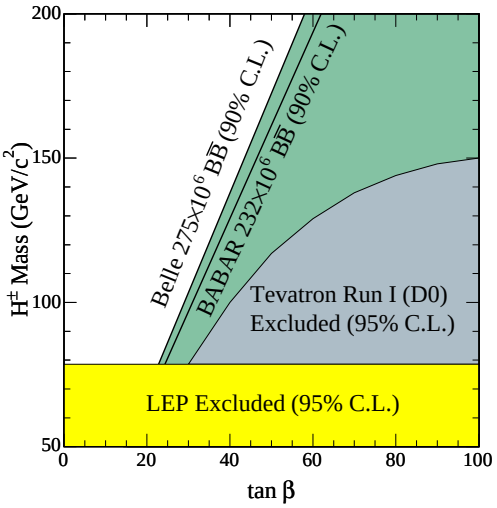

FIG. 5: The 90% C.L. exclusion boundaries in the $[M_{H^+}, \tan\beta]$ plane obtained from the observed upper limit on $\mathcal{B}(B^- \to \tau^- \nu)$.

we get an upper limit on $\mathcal{B}(B^- \to \tau^- \overline{\nu})$, we can give a constraint on $\tan\beta$ and m_H. Fig. 5 shows the 90% C.L. exclusion boundaries in the $[m_H, \tan\beta]$ plane obtained with $m_B = 5279$ MeV/c^2 and $\mathcal{B}(B^- \to \tau^- \overline{\nu})_{\rm SM} = 0.93 \times 10^{-4}$ from the CKMfitter prediction compared with other experimental searches at LEP[16], at the Tevatron[17], and at BABAR.

In conclusion, we have performed a search for the $B^- \to \tau^- \overline{\nu}$ and $B^- \to K^- \nu \overline{\nu}$ decays in a fully reconstructed B sample. Upper limits have been set :

$$\mathcal{B}(B^- \to \tau^- \overline{\nu}) < 1.8 \times 10^{-4} \quad (90\% \text{ C.L.}) \tag{8}$$

$$\mathcal{B}(B^- \to K^- \nu \overline{\nu}) < 3.6 \times 10^{-5} \quad (90\% \text{ C.L.}) \tag{9}$$

which are the most stringent upper limits on these processes to date.

We thank the KEKB group for the excellent operation of the accelerator, the KEK cryogenics group for the efficient operation of the solenoid, and the KEK computer group and the National Institute of Informatics for valuable computing and Super-SINET network support. We acknowledge support from the Ministry of Education, Culture, Sports, Science, and Technology of Japan and the Japan Society for the Promotion of Science; the Australian Research Council and the Australian Department of Education, Science and Training; the National Science Foundation of China under contract No. 10175071; the Department of Science and Technology of India; the BK21 program of the Ministry of Education of Korea and the CHEP SRC program of the Korea Science and Engineering Foundation; the Polish State Committee for Scientific Research under contract No. 2P03B 01324; the Ministry of Science and Technology of the Russian Federation; the Ministry of Higher Education, Science and Technology of the Republic of Slovenia; the Swiss National Science Foundation; the National Science Council and the Ministry of Education of Taiwan; and the U.S. Department of Energy.

[1] J. Charles *et al.* (CKMfitter Group), Eur. Phys. J. C **41**, 1 (2005) and the updated results presented at CKM2005 workshop.
[2] B. Aubert (BABAR Collaboration), arXiv:hep-ex/0407038.
[3] Y. Grossman, Z. Ligeti and E. Nardi, Nucl. Phys. B **465**, 369 (1996) [Erratum-ibid. B **480**, 753 (1996)] [arXiv:hep-ph/9510378].
[4] C. Bird, P. Jackson, R. Kowalewski and M. Pospelov, Phys. Rev. Lett. **93**, 201803 (2004) [arXiv:hep-ph/0401195].
[5] A. Faessler, T. Gutsche, M. A. Ivanov, J. G. Korner and V. E. Lyubovitskij, Eur. Phys. J. directC **4**, 18 (2002) [arXiv:hep-ph/0205287].
[6] G. Buchalla, G. Hiller and G. Isidori, Phys. Rev. D **63**, 014015 (2001) [arXiv:hep-ph/0006136].
[7] B. Aubert *et al.* (BABAR Collaboration), Phys. Rev. Lett. **94**, 101801 (2005) [arXiv:hep-ex/0411061].
[8] S. Kurokawa and E. Kikutani, Nucl. Instrum. Methods Phys. Res., Sect. A **499**, 1 (2003)
[9] Belle Collaboration, A. Abashian *et al.* Nucl. Instrum. Methods Phys. Res., Sect. A **479**, 117 (2002)
[10] H. Albrecht *et al.* (ARGUS Collaboration), Phys. Lett. B **185**, 218 (1987).
[11] E. D. Bloom and C. Peck, Ann. Rev. Nucl. Part. Sci. **33**, 143 (1983).
[12] R. Brun *et al.*, GEANT3.21, CERN Report DD/EE/84-1 (1984).
[13] See the EvtGen package home page, http://www.slac.stanford.edu/∼lange/EvtGen/.
[14] F. James and M. Roos, Comput. Phys. Commun. **10** (1975) 343.
[15] W. S. Hou, Phys. Rev. D **48**, 2342 (1993).
[16] P. Bock *et al.* (ALEPH, DELPHI, L3 and OPAL Collaborations), CERN-EP-2000-055
[17] V. M. Abazov *et al.* (D0 Collaboration), Phys. Rev. Lett. **88**, 151803 (2002) [arXiv:hep-ex/0102039].